Solution of Seismic Source Function in Near-Field from High-Speed Train and Energy Characteristic Analysis

baoxin Jia[1] and Wenya Yuan[1]

[1]Liaoning Technical University

November 21, 2022

Abstract

The solution to high-speed-railway seismic source function is of great theoretical significance for the inversion of high-speed-railway focal mechanism, propagation law and energy evolution, which may provide a reference for the seismic exploration of rock mass structure in shallow ground. In this paper, the simulation signal characteristic is studied through MATLAB, by working out the Green function of high-speed ailway seismic source in near-field and proceeding forward calculation. Based on the comparative analysis of simulation signal and measured data, the Green function is verified. In addition, wth further analysis of vibration curves, frequency-spectrum diagrams and energy distribution maps, the results show that in the near-field of high-speed railway seismic source: The seismic signal is broadband, of which the vibration differences at each observation position in the horizontal direction indicate the propagation law of high-speed railway seismic wave, while the energy attenuation characteristic can be reflected by that in the vertical direction; There are clear discrete spectral lines in high-speed railway seismic wave, of which the feature frequency varies from 60Hz to 370Hz, affected by the propagation distance; The spacial energy distribution of high-speed railway seismic wave radiation in near field depends on the frequency response property at the seismic source, and the frequency response property shows significant difference with the frequency ranging from 40Hz to 500Hz.

Hosted file

`essoar.10511432.1.docx` available at https://authorea.com/users/528821/articles/596951-solution-of-seismic-source-function-in-near-field-from-high-speed-train-and-energy-characteristic-analysis

1. X. Jia[1, 2], W. Y. Yuan[1]*

[1] School of Civil Engineering, Liaoning Technical University, Fuxin 123000, China

[2] Liaoning Key Laboratory of mine subsidence disaster prevention and control, Liaoning Technical University, Fuxin 123000, China

Corresponding author: Wenya Yuan (ywenia@163.com)

Key Points:

- The high-speed railway seismic source model in nearfield is established with the Green function solved and verified.
- The propagation attenuation behaviors of high-speed railway seismic wave are related to the propagation direction.
- The energy radiation characteristic of high-speed railway seismic shows obvious difference from 40Hz to 500Hz.

Abstract

The solution to high-speed-railway seismic source function is of great theoretical significance for the inversion of high-speed-railway focal mechanism, propagation law and energy evolution, which may provide a reference for the seismic exploration of rock mass structure in shallow ground. In this paper, the simulation signal characteristic is studied through MATLAB, by working out the Green function of high-speed ailway seismic source in near-field and proceeding forward calculation. Based on the comparative analysis of simulation signal and measured data, the Green function is verified. In addition, wth further analysis of vibration curves, frequency-spectrum diagrams and energy distribution maps, the results show that in the near-field of high-speed railway seismic source: The seismic signal is broadband, of which the vibration differences at each observation position in the horizontal direction indicate the propagation law of high-speed railway seismic wave, while the energy attenuation characteristic can be reflected by that in the vertical direction; There are clear discrete spectral lines in high-speed railway seismic wave, of which the feature frequency varies from 60Hz to 370Hz, affected by the propagation distance; The spacial energy distribution of high-speed railway seismic wave radiation in near field depends on the frequency response property at the seismic source, and the frequency response property shows significant difference with the frequency ranging from 40Hz to 500Hz.

Plain Language Summary

High-speed railway seismic refers to the vibration caused by wheel-rail contact between the high-speed train and track, which is regarded as repeatable artificial seismic source recently. In this paper, the simulation signal characteristic is studied through MATLAB, by working out the Green function of high-speed ailway seismic source in near-field and proceeding forward calculation. At the

same time, the vibration curves and frequency amplitude spectrum of simulationl signal are analyzed through Fourier transform, of which the results show consistency with that of both the measured data and previous study results, followed with energy radiation characteristic analysis. Therefore, the reliability of the solution to the Green function is verified, which is expected to provide theoretical guidance for exploring the propagation law and energy evolution characteristics of high-speed-railway seismic wave, and may provide a reference for the seismic exploration of rock mass structure in shallow ground.

Keywords High-speed Railway Seismic; Green Function; Simulation Analysis; Frequency Spectrum; Energy Distribution;

1. Instruction

With the rapid development of high-speed railway construction and the increasingly operating mileage of high-speed train, the vibration impact caused by high-speed train is more and more prominent(Li et al, 2007; Kouroussis et al, 2014; Galvín et al, 2009; Takemiya et al. 2007), which may result in vibration damage to railway engineering structures such as viaducts, and also pose a great threat to the safe operation of high-speed train. It is noteworthy that in engineering, the new problems of track system are mostly caused by different degrees of high-frequency vibration above 20Hz(Chen Z S et al, 2004), which are mainly distributed in the near-field term of high-speed railway seismic source(Li L et al, 2004). As a result, solving the Green function in the near-field from the high-speed railway seismic source is crucial to exploring the propagation law and energy evolution mechanism of high-speed railway seismic wave and developing a further research on vibration response of railway engineering structure.

The research in the field of high-speed railway seismic around the world is gradually carried out since the 21st century, With the gradual deepening of which people pay more attention to the particularity of both the load form of high-speed train and signal characteristics of high-speed railway seismic. Depending on the vibration data of the new high-speed railway section from Brussels to Paris, G. Degrande's team(Lombaert et al, 2001; Degrande and Schillemans, 2001) have demonstrated the applicability of the improved Krylov prediction model ,which is available for numerical analysis of high-speed train, as moving load. L. Auersch(Auersch L, 2006) proposed that the moving dynamic loads of a train are approximated by fixed dynamic loads, and the propagation of waves through homogeneous or layered soil is calculated based on the half-space theory. In simulation analysis, Katou(Katou et al, 2008) took the force on the wheel of running train into considerition and the ground vibration caused by Shinkansen train is studied by discrete and finite FDM simulation.Also, the equidistant spectral characteristics of train vibration signal are found by F. Fuchs and G.Bokelmann(Fuchs et al, 2017). In order to explore the influence factors of seismic signal induced by high-speed train, academician Zhai Wanming(Zhai et al, 2015) and her team carried out vibration test along Beijing-Shanghai high-speed railway, and analysed the relationship between the high-speed train speed with the characteristic of ground vibration acceleration in the domain of time and frequency, with high-speed train running on ballastless track.

In addition, since the "Coordination Office of High-speed train seismology Research" founded in 2018, which is subordinate to the institute of Geology and Geophysics, Chinese Academy of Sciences, quite a few experts find that the high-speed railway seismic signal is rich in low frequency, which is conducive to geological prospecting. A lot of scientific research achievements have been acquired in high-speed train seismology fields(Zhang et al, 2019; Wang et al, 2021; Zhang et al, 2019), including source model, source time function, real-measured data processing, signal modeling and imaging technology. It is noteworthy that the moving high-speed train is mathematically simplified and modeled as a moving-line source(Cao and Chen, 2019), under the action of which the calculations of Green function in far-field of elastic half space and space are given, diacarding the slight influence of force source position on the numerical value of r and $_{i}$. However, the simplified method is approximate only in case of the high-speed railway seismic in near field, where the distance from the position of the force source on the high-speed railway line source to the observation position is far greater than the length of the train. When the observation position is close to the high-speed train seismic source, that is in the near-field, the length of moving-line source has such a great influence on r and $_{i}$ that it may cause obvious deviation between the simulated signals and the measured data in the following analysis of the frequency response and radiation energy distribution of the high-speed railway seismic source function in near-field.

In this article, we solving the Green function in near-field, with taking the numerical influence of high-speed train's length on propagation distance of high-speed railway seismic signals into consideration and correcting the propagation distance to a variable related to running time and force source position at high-speed train, which raised accuracy of calculation results further. Meanwhile, frequency spectrum and radiant energy spatial distribution of high-speed railway seismic signal are analyzed by Fourier transform, which may lay a theoretical foundation for the study on propagation law and energy evolution mechanism of high-speed railway seismic wave.

2. Modeling and Solution of the high-speed railway Seismic Source

In order to analyze the energy radiation characteristics of high-speed railway seismic wave directly under the viaduct and further explore the dynamic response characteristics of elevated piers as well as relevant foundation structure under high-speed railway seismic, the simplified seismic source model is established, which is helpful to understand the position relationship between the high-speed railway seismic source and each observation station, as shown in Figure 1. The spacial rectangular coordinate system is built as taking the central position of train head as the coordinate origin, the direction parallel to the running direction of high-speed train as the positive direction of x-axis, the downward direction perpendicular to the ground surface as the positive direction of z-axis. It is assumed that the force source act along the posotive direction of z-axis merely, the propagation medium underground being homogeneous and the running state being consistent.

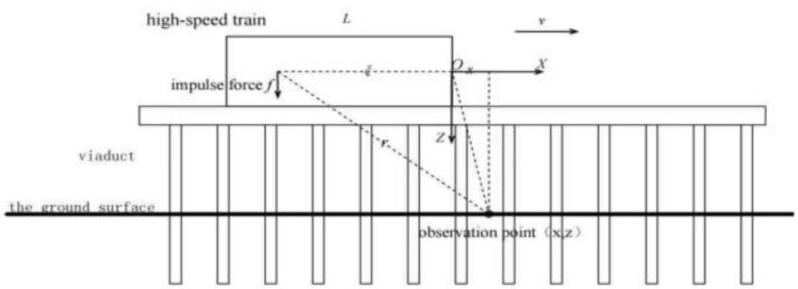

Figure 1 Simplified model of high-speed train seismic source in near-field

In order to analyze the near-field vibration response characteristics of high-speed railway seismic, referring to the Green function in the infinite uniform complete elastic space(Aki and Richards, 2002) and the Green function of moving-line source in half space(Cao and Chen, 2019), based on the simplified model shown in Figure 1, we obtain the near-field term of Green function in infinite uniform complete elastic space of high-speed train moving-line sismic source through preliminary integration.The function solved is as follows:

(1)

where x is the horizontal coordinate value of the observation position; $r( )$ is the distance from the position of the force source on the high-speed railway line source to the observation position; t is the operation time of high-speed train; *is* the density of the propagation medium; L is the length of the high-speed train; $_i$ is the direction cosine related to vector x; $_n$ is the direction cosine related to impulse force f; is the delta function; is the wave velocity of P-wave; is the wave velocity of S-wave; v is the running speed of high-speed train; is the action time of unit concentrated impulse; is the distance from the force source to the head of the high-speed train.

Besides, the radiation pattern of high-speed railway seismic wave is represented by R, which can be expressed as:

(2)

Owing to the decisive role in the directional characteristics of energy radiation from high-speed railway seismic source, the value of R can be used to represent the displacement radiation characteristics produced by the initial motion of high-speed railway seismic wave on the ground.

By using the symmetry and sampling properties of the delta function, the Formula (1) can be simplified. When the conditions of and are met at the same time, the Green function in near-field term of high-speed railway moving-line source can be expressed as:

(3)

The displacement function can be obtained by convoluting the Green function with the time function , expressed as:

(4)

which is used to describe the vibration of the moving-line source at different time points.

Since the distance from the force source to the observation position is short enough in the near-field range, that both the influence of the high-speed train running time and the force source position on the propagation distance of high-speed railway seismic wave should be considered in the numerical calculation, that is,

(5)

where z is the coordinate value perpendicular to the ground surface of the observation position. At the same time, $_i$ and $_n$ can be expressed as:

(6)

Taking the Equation (4) and Equation (5) into Equation (2), therefore we can obtain the Green function in near-field of high-speed railway moving-line seismic source as follows:

(7)

As to reflect the stress condition of the track and the wave field characteristics on the ground surface accurately, the source time function in box-term is selected for solution[18], as follows:

(8)

where *H(t)* is the step function.

After Integration, Equation (7) is transfered into

(9)

the value of which can represent the vibration degree of observation points under continuous impulse of high-speed railway seismic source. Meanwhile, it can be applied to analyzing the frequency spectrum of high-speed railway seismic wave and the spatial distribution characteristics of radiation energy.

3. Verification of the high-speed railway seismic source function in near-field

In order to analyze the frequency-spectrum and energy distribution of high-speed railway seismic signal, we transform the near-field term of high-speed railway seismic source function from time-domain to frequency-domain solved in section 1 by Fourier transform. The modulus of equation (9) can be caculated without considering the phase change, as follow:

(10)

where the   is the feature frequency and the modulus of the Green function can be used for forward calculation and signal analysis of high-speed railway seismic wave. The parameters of numerical calculation are set as follows: the length of high-speed train is, That is, the train has 8 carriages; the running speed of the high-speed train is ; the density of medium underground is ; the velocity of *P*-wave and *S*-wave is and respectively.

Based on the displacement function shown in Equation (3), the theoretical value of high-speed railway seismic events in both the positive direction of *z-axis* and *z=5* can be caculated, by convoluting the Green function of high-speed railway seismic source in near field shown in Equation (9) with the source time function shown in Equation (7). There are four observation points selected in each direction as A_1, A_2, A_3, A_4 and B_1, B_2, B_3, B_4 respectively. The distances between adjacent observation points in the same direction differentiate with each other, and the distances between any adjacent observation points in each direction is consistent with that in the other direction.The distribution diagram and the spatial coordinate of each theoretical observation position are shown in Figure 2 and Table 1 respectively.

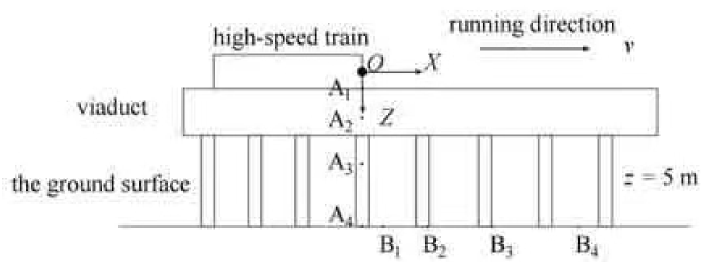

Figure 2 Map of simulation signal observation point

Table 1 The coordinate of each observation point

Point	Coordinate	Point	Coordinate
A_1	(0 5m)	B_1	(5m 5m)
A_2	(0 15m)	B_2	(15m 5m)
A_3	(0 30m)	B_3	(30m 5m)
A_4	(0 55m)	B_4	(55m 5m)

3.1 The vibration curve of simulation signal

The vibration curves of simulation signal in the directions of *z*-axis and *z*=5 are drawn by MATLAB, which is shown in Figure 3 (a) and Figure 3 (b) as follows. When t=0, the head of high-speed train is defined to be located at the coordinate origin of plane rectangular coordinate system (as shown in Figure 1).

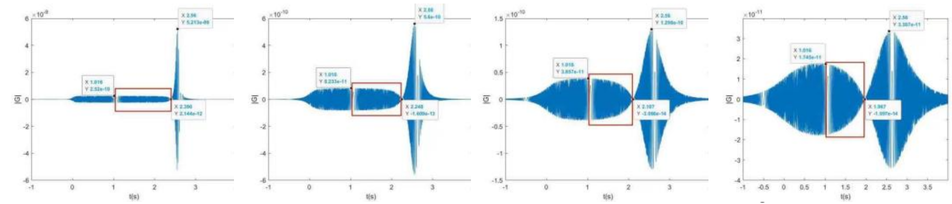

A4

A1 A2

(a) The positive direction of *z-axis*

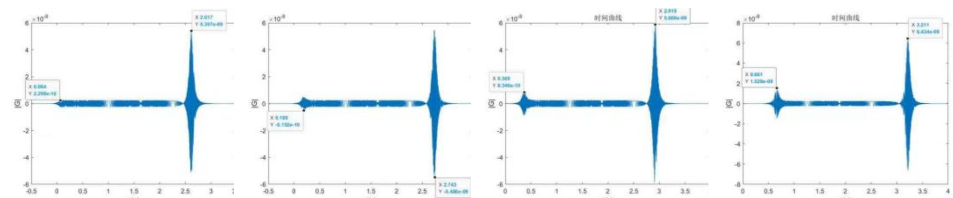

B4

(b) The positive direction of *z=5*

Figure 3 Vibration curve of simulation signal

As shown in Figure 3 (a), it can be seen that all the maximum value of each vibration curve appear at approximately 2.6 s when the x coordinate value of the observation position is fixed. As calculated from the preset length of high-speed train and its running speed, it takes exactly about 2.6 s for the high-speed train to pass the origin completely. Therefore, it can be interpret that the vibration peak value appears at the moment that the high-speed train passes the observation position completely. Also through the analysis of Figure 3 (b), the vibration curves possess the characteristics of double peaks in different degrees, which are named as the first peak and the second peak in time sequence. When the z-coordinate value of the observation point is fixed, with the x-coordinate value increasing, the double-peaks characteristic of the vibration curves becomes more obvious and the appearence time of both maximums is postponed gradually. Significantly, the first peak appears when the high-speed train just arrives at the position on x-axis corresponding to each observation point in each figure and the time difference between the two peaks is always approximately 2.6s, exactly in accordance with the time required for the high-speed train to completely pass through an observation point. Therefore, according to the time-domain characteristic of vibration curves in the posotive direction of *z-axis* and line *z=5*, the reliability of high-speed railway seismic source function solved in section1 is verified preliminarily.

Besides, the vibration curves in the four graphs of Figure 3 (a) are weakened in a short time after 1.02 s, of which the starting time and ending time are 1.02s-2.40s, 1.02s-2.25s, 1.02s-2.11s and 1.02s-1.97s respectively. Influenced by the propagation distance, the attenuation duration decreases gradually with the coordinate value of *z-axis* increasing, which may due to that the phenomenon of wave interference accurs when the difference value of propagation distances from two waves to the observation point is the odd times of the wavelength, as the high-speed railway train passing through the observation position.And the vibration cancellation appears when the phases of two columns of interference waves are opposite, which is shown as vibration attenuation in the Figure 3 (a). As showing, the half length of the train passes through the coordinate origin at around 1.02s, consistent with the time when the distances from the symmetrical force source positions on both sides of the *z-axis* to the observation point on the *z-axis* are approximately the same, causing the energy value of high-speed railway seismic wave from the symmetrical force source positions being approximately the same at the observation point. Among them, the energy counteraction of some signal that meet the conditions of waves interference with opposite phases occurs almost entirey, which explains the reason for the obvious attenuation in the vibration curves. However, with the high-speed train passing through compeletely, the energy difference between two columns of interference waves from both sides of the *z-axis* increases gradually. Since the vibration cancellation degree only depends on the signal wave with less energy and the residual energy without cancellation in the signal wave with large energy is retained, the vibration amplitudes of four vibration curves increase gradually after 2.4s, 2.25s, 2.11s and 1.97s respectively. And it is speculated that the bimodal characteristic in Figure 3 (b) is affected by the length of the high-speed train. That is, the high-speed railway seismic wave excited at different force source positions propagates to the same observation position with different time required, among which the maximum value of time difference is just the time required for the seismic wave to propagate from the end of the train to the head, just about 2.6s.

At the same time, by comparing the characteristics of two groups of vibration curves in the positive direction of both *z-axis* and line $z{=}5$, it can be seen that the bimodal characteristic difference of vibration curves at different observation positions in the positive direction of line $z{=}5$ reflects the propagation law of high-speed railway seismic source wave, and the energy attenuation characteristic can be reflected by the differences of vibration curves in the positive direction of *z-axis*. However, the paper is designed to solve and verify the high-speed railway seismic source function in near-field, followed with energy radiation characteristic analysis of high-speed railway seismic wave under the viaduct on this basis. As a result, the energy attenuation mechanism of vibration signal in Figure 3 (a) and the signal propagation law based on the bimodal characteristic of vibration curve in Figure 3 (b) will not be discussed in detail, and the related problems remain to be studied further.

3.2. Spetrum characteristic analysis of simulation signal

In order to explore the main energy distribution in frequency of high-speed railway seismic wave in near-field, based on the simplified model and relevant assumptions of high-speed railway seismic source function, we substitute the preset value of the parameter into Equation (10) for forward modeling caculation. The amplitude-frequency diagram from six observation points with different propagation distances are drawn by MATLAB software with the sampling frequency set to 10kHz, shown as Figure 4, of which the abscissa represents the frequency and the ordinate is the amplitude of the simulation signal of high-speed railway seismic wave.

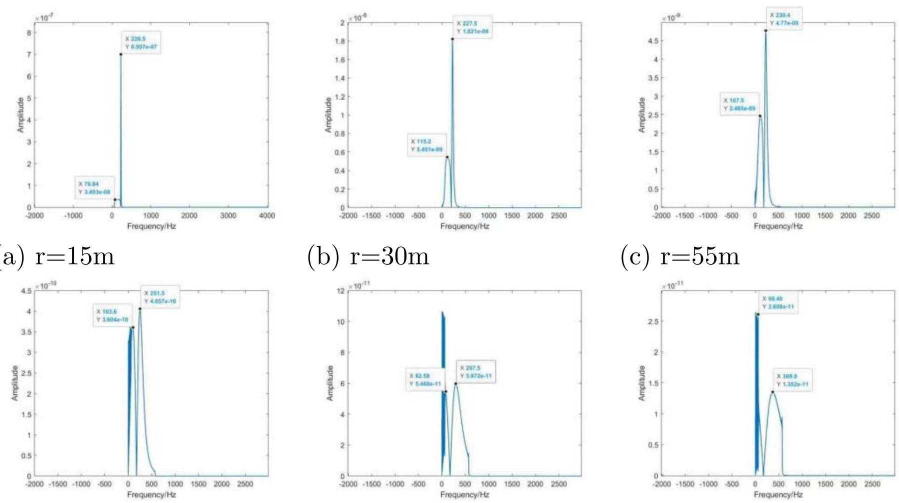

(a) r=15m (b) r=30m (c) r=55m

(d) r=150m (e) r=300m (f) r=500m

Figure 4 The amplitude-frequency diagram of simulation signal from differert observation points

As Figure 4 describing, the amplitude frequency diagrams of six group of simulation signal are characterized with discrete spectral lines, which is consistent with the previous research conclusion that there are obvious narrow-band discrete spectral lines in the vibration signals from train running on track(Wang et al, 2019; Wen et al,2019; Bao et al, 2019;Hu et al, 2019). It can be seen that there are two narrow-band in the each diagram.The frequency at the peak of the discrete narrow-band is defined as the feature frequency, of which the smaller part in each diagram is named as the first feature frequency with the larger part named as the second feature frequency.

It can be seen from the Figure 4 that the first feature frequency in each diagram are approximately 92Hz, 121Hz, 108Hz, 104Hz, 83Hz and 60Hz respectively, while the second feature frequency are approximately 227Hz, 227Hz, 230Hz, 252Hz, 298Hz and 370Hz respectively. Taking 50m as the dividing distance, when the propagation distance is less than 50m, the value of the first feature frequency gradually increases with the propagation distance increasing, while when the propagation distance is more than 50m, the first feature frequency gradually decreases. While the second feature frequency increases all the time with the propagation distance of high-speed railway seismic wave increasing. At the same time, with the propagation distance increasing, the amplitude of high-speed railway seismic simulation signal decreases gradually under both two feature frequencies. Taking 150m as the dividing distance, when the propagation distance is less than 150m, the amplitude of the high-speed railway seismic simulation signal under the second feature frequency is larger than that of the first feature frequency, while when the propagation distance is more than 150m, the amplitude of the high-speed railway seismic simulation signal under the second feature frequency is smaller than that of the first feature frequency. Therefore, the amplitude attenuation of high-speed railway seismic simulation signal is faster under the second feature frequency.

As a result, it can be concluded that the feature frequency and amplitude attenuation of high-speed railway seismic simulation signal at each observation point are influenced by the propagation distance of high-speed railway seismic wave. Due to the damping effect of the medium, the energy attenuation of high-speed railway seismic wave always occurs in the process of propagation, which explained the reason for the amplitude reduction of high-speed railway simulation signal under both two feature frequencies in Figure 4 with the propagation distance increasing. Due to the fact that the frequency and spectrum of the medium-high frequency signal wave propagates with faster attenuation degree and faster attenuation speed, the first feature frequency gradually decreases when the propagation distance is more than 50m and the amplitude under the second feature frequency drops faster than that of the first feature frequency when the propagation distance is morer than 150m.

4. Field Measurement and Data Analysis

In order to verifying the reliability of the Green function in near-field from the high-speed railway seismic source solved in Section 1, we collected high-speed railway seismic signals near Fuxin station in Beijing-Shenyang section, of which the total length is 696 *km* with a designed speed of 350 *km/h*, of Beijing to Harbin high-speed railway, being a section part of Beijing-Harbin high speed railway from Beijing Chaoyang Station to Shenyang station.

4.1 Site selection and station layout

The field test of vibration signal monitoring and storage are carried out along Beijing-Shenyang high-speed railway, in Dongwazi village, Sihe Town, Fuxin City, Liaoning Province, where it is sparsely populated. The longitude of the monitoring sites ranges from 42°05'29.73"N to 42°05'36.96"N, while the latitude ranges from 121°63'26.43" E to 121°63'29.31" E. There is almost no background noise interference, such as industrial noise and domestic noise, and conducive to vibration signal monitoring of high-speed railway seismic. The distribution of stations and the position of high-speed railway site is shown in the map below as Figure 5.

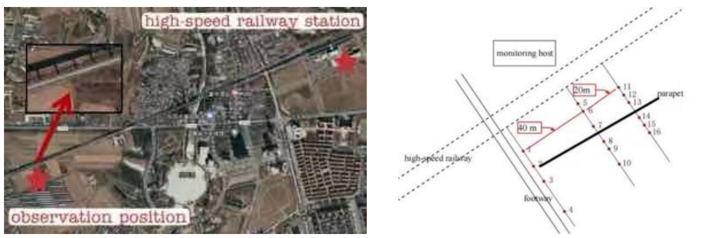

Figure 5 Distribution of the high-speed railway and stations

The sixteen sensors are buried in the soil on ground surface and laied out from the near to the distant to collect vibration signals under the viaduct, which is about 5 meters above ground level, and the field test situation is shown in Figure 6.

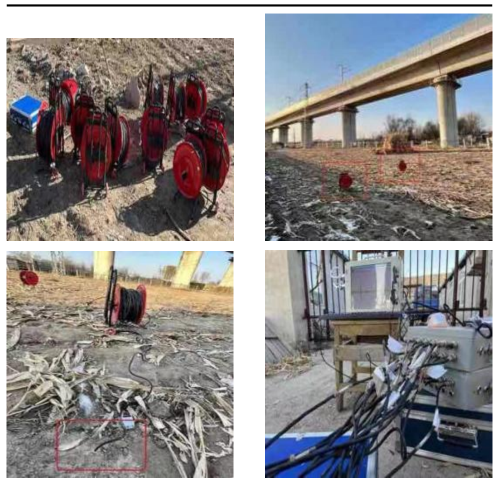

Figure 6 The field test condition of vibration signals collection

4.2 Test equipments and parameters

In the field test, Antenna-III is used to monitor and collect the real-time vibration data, whose magnitude monitoring ranges from -3 to 2. The equipment is mainly composed of five parts including host machine, sensors(or detectors), converters, hubs and cables, with data storage capacity being 32 GByte + 2000

GBytes, external interface of data transmission being USB2.0, interface of wired network being RJ45, and it works with the continuous acquisition system. Besides, one side of the hub is connected to the sensors by cables, while the other connected to the host machine through a converter and a special data transmission line. The high-speed railway seismic signal monitoring and acquisition start after both the host machine and hub are powered on at the same time. The detailed parameters of test equipments are shown in Table 2.

Table 2 Parametes of the test equipment

Equipment	Quantity	Notes
Sensor/Detector	6	the sensitivity is100 V/(m/s) and the sampling frequency is up to 100kHz
Cable	6	about 200 meters long per reel
Hub	1	including12 data channels
Concerter	1	worked at the voltage of DC12V or 220V merey
Host machine	1	used to monitor and store the target vibration data

4.3 Spectrum analysis of the measured data

In order to further verify the Green function solved in part 1, based on the simulation analysis of high-speed railwayseismic signals frequency-spectrum characteristic under different propagation distances and the feasibility of field monitoring test, the frequency spectrum of measured data from high-speed railway seismic wave monitored by observation point numbered 1, 3 and 4 are drawn by MATLAB, of which the distances from the stations to the seismic source are the same as that of simulation signals named (a), (b) and (c) respectively, as shown in Figure 7.

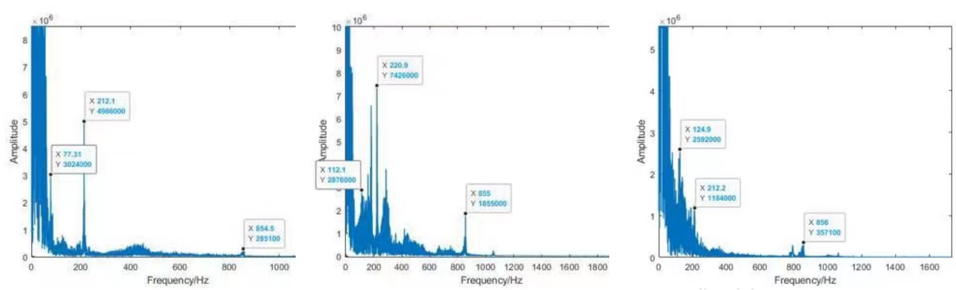

Number 1 r=15m   2 r=30m   Number 4 r=55m

Figure 7 Frequency-spectrum of measured data from high-speed railway seismic wave

As shown in Figure 7 (a), (b), there are obvious discrete spectral lines in the amplitude-frequency diagram of the measured signals when the propagation distance is 15 m and 30 m, while the discrete spectral characteristic gradually weaken with the propagation distance increasing to 55 m, as shown in Figure 7 (c). Therefore, it can be concluded that with the propagation distance increasing, the discrete spectral lines of high-speed railway seismic signals collected on site become unclear gradually. In addition, the typical characteristic as narrow-band discrete spectral lines of high-speed railway seismic signals measured in the near-field is consistent with previous analysis results of other researchers(Jiang et al, 2019; Liu and Jiang, 2019; Jiang et al, 2019; Wang et al, 2019; He et al, 2007; Sheng et al, 2004), in the case of which the accuracy of the numerical analysis is confirmed.

It can be seen that there are three discrete spectral lines in each drawing of figure 7, and the obvious degree of discrete spectral lines is different among them. The feature frequencies are approximately 77Hz, 212Hz, 855Hz in Figure 7 (a), 112Hz, 221Hz, 855Hz in Figure 7 (b) and 125Hz, 209Hz, 791Hz in Figure 7 (c). As the propagation distance increasing, the first feature frequency goes higher ranging from 70 Hz to 130 Hz, of which the corresponding amplitude decreases gradually; the second feature frequency increases first and then decreases ranging from 200 Hz to 220 Hz, of which the corresponding amplitude increases first and then decreases as well; the third feature frequency is almost stable around 855 Hz without significant change, of which the corresponding amplitude increases first and then decreases.

Therefore, the variation range of the first two feature frequency in the field measured data is close to that of the first feature frequency and the second feature frequency in the simulated signals respectively, through which the seismic source model and function solution of high-speed railway in near-field is verified furthermore. At the same time, it lays a theoretical foundation for the simulation analysis of frequency response characteristic and energy distribution characteristic in high-speed railway seismic wave field.

However, due to the fact that there are some differences between the preset value and the actual parameters of propagation medium, as well as the complex propagation mechanism of the high-speed railway seismic wave such as reflection, refraction and resonance, the feature frequency value and amplitude changing tendency from the seismic signals obtained by high-speed railway seismic signal forward calculation and field acquisition can not be completely consistent.

5. Energy distribution analysis of high-speed railway seismic wave field

According to the spectrum characteristic of the simulated data in Section 2 and the measured data in Section 3, it can be seen that the two group of feature frequencies of high-speed railway seismic wave in the near-field vary from 60 Hz to 120 Hz and 230 Hz to 370 Hz respectively. Owing to the fact that the operation time of high-speed train only causes the phase change of simulation signal, yet hardly affects the energy distribution characteristics of high-speed railway seismic wave field. As a result, Equation (9) is used to calculate the frequency response of the moving-line seismic source in near-field at $t = 0$.

Shown as figure 8 , the spatial energy distribution diagrams on the x-o-z plane of high-speed railway seismic wave are drawn at 1Hz, 40Hz, 60Hz, 120Hz, 230Hz, 270Hz, 500Hz and 1000Hz. According to the energy spectrum, the tone goes warm in the figure with the radiation energy value gradually increasing.

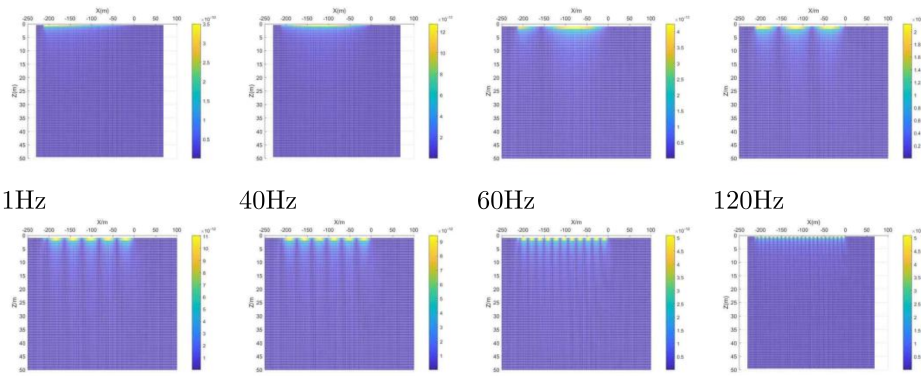

1Hz 40Hz 60Hz 120Hz

230Hz 270Hz 500Hz 1000Hz

Figure 8 The energy distribution of high-speed railway seismic wave at different frequencies

5.1 Distribution characteristic of radiant energy

Through comprehensive analysis of each graph in figure 8, the energy of high-speed railway seismic reaches maximum at line-source, and radiates outwards from the line-source. In the horizontal direction of spatial coordinates, the high-speed railway seismic wave energy is concentrated in the range of - 220 m to 0, which is determined by the perset coordinate position of the simplified model (shown as Figure 1) and length of high-speed train. While in the vertical direction of spatial coordinates, the energy characteristics of high-speed railway seismic waves at various locations in space are mainly determined by the energy at the point of line-source with the same abscissa values, and attenuates with the vertical distance from line source increasing. From the above mentioned, therefore, it can be concluded that the energy radiation characteristics in high-speed railway seismic wave field depend on the energy distribution on the line-source.

5.2 Frequency response characteristics analysis

It can be seen from the comparison of each diagram in Figure 8 that there are obvious differences in spatial energy distribution of high-speed railway seismic wave at different frequencies, especially at the line-source: The energy distribution at the line-source is continuous but non-uniform at the frequency range from 1Hz to 40Hz. As the frequency increasing, the energy distribution at the line-source turns uniform gradually with more discontinuity points. When the frequency is higher than 500Hz, the energy distribution characteristics of high-speed railway seismic wave field under different frequencies are mainly represented in the number of energy discontinuity points at the line source, and both the radiation energy as well as its distrubution range in the wave field turn smaller with the distance to seismic source increasing. As a result, it can be concluded that the frequency response characteristics of high-speed railway seismic wave in the near-field are mainly determined by the signals within the frequency range of 40-500Hz, and according to analysis of the simulated signals in Section 2 the measured data in Section 3, it contains almost all feature frequency in the near-field of high-speed railway seismic source.

6. Discussion

The spatial distribution diagrams of high-speed railway seismic wave energy radiation characteristics at 1 Hz are drawn in Figure 9 (a), (b) and (c) by defining the value of radiation pattern as, and respectively.

1Hz

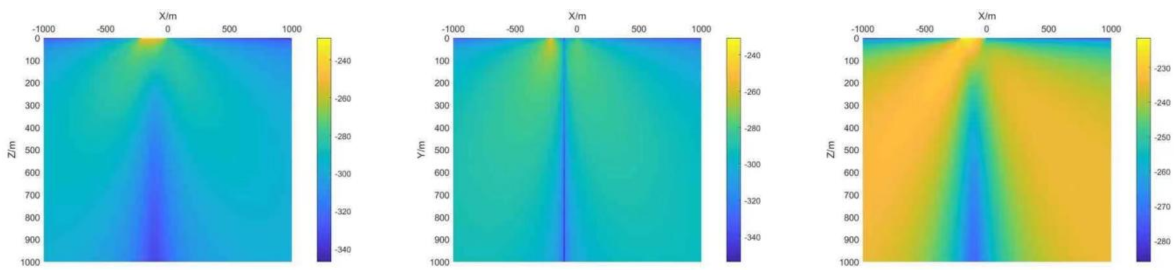

(a) $R = \ _{i\bullet}\ _{n}$ (b) $_{i} = 1\ R = \ _{n}$ (c) $_{n} = 1\ R = \ _{i}$

Figure 9 The radiation energy spatial distribution characteristic under different value of radiation pattern

According to the comprehensive analysis of each figure, affected by the line-source characteristic of the high-speed railway seismic, it can be seen that there is a sudden decrease in energy near the vertical line of the moving-line seismic source. By comparing the radiation energy spatial distribution characteristic of P-wave and S-wave in the far-field term of Green function from high-speed railway seismic source [17] with Figure 9 (b), (c), it can be found that the radiation energy spatial distribution characteristic in near-field is similar to that of P-wave in far-field when taking, while similar to that of S-wave in far-field when taking .

Considering the fact that the energy distribution of high-speed railway seismic wave field depends on the comprehensive radiation effect of P-wave and S-wave and combining the directionality of propagation feature of P-wave and S-wave, it can be inferred that $_n$ mainly reflects the energy radiation characteristic of P-wave, and the energy radiation characteristic of S-wave is determined by $_i$. However, based on the Green function in near-field from the high-speed railway seismic source, whether it is available for exploring the propagation law of P-wave and S-wave respectively by adjusting the relevant value of radiation pattern remains to be further explored.

According to the relative spatial position from observation point to high-speed railway seismic source and the directionality of propagation feature of P-wave and S-wave, if the assumption holds, it may help to study the propagation law and energy attenuation of P-wave and S-wave respectively, as well as to deeply analyze the vibration response of theobservation point under P-wave and S-wave respectivly, which may provide new idea for the study of antiseismic structure form and material selection under high-speed railway.

7. Conclusion

By establishing the high-speed railway seismic source medel in near-field and solving the Green function, the research on the simulation signal characteristic is conducted on the basis of forward calculation by MATLAB. As a result, the reliability of the solution to high-speed-railway seismic source function in near field is verified by comparing the characteristic of simulation signal with that of the measured data generated by high-speed train, which may provide reference for dynamic response study of high-speed railway engeneering structure and further exploration of rock mass structure in shallow earth. According to the simulation signal characteristic analysis including the vibration curve, frequency spectrum and energy radiation, the results show that in the near-field of high-speed railway seismic source:

(1)The simulation signal is broadband, among which the differences of vibration curves at each observation position in the horizontal direction indicate the propagation law of high-speed railway seismic wave, while the energy attenuation characteristic can be reflected by the differences of vibration curves at different each position in the vertical direction;

(2)The simulation signal appears with clear discrete spectral lines, of which the feature frequency varies from 60Hz to 370Hz, affected by the propagation distance of high-speed railway seismic wave;

(3)The spacial energy distribution of high-speed railway seismic wave radiation in near field depends on the frequency response property at the seismic source, and with the frequency ranging from 40Hz to 500Hz.

As the wheel-rail contact between the high-speed train and the track actually appears in both horizontal and vertical directions, therefore, the radiant energy of high-speed railway seismic wave in space is determined by both vertical force and lateral force. Considering the dominant effect of wheel-rail contact in vertical direction, the Green function in near-field from the high-speed railway seismic source is solved, based on the assumption that the force from wheel-rail contact only acts in the positive direction of *z-axis*. On this basis, the influence of lateral force impact on the radiation energy in near-field under the high-speed railway source should be considered in the future.

Acknowledgments

- The work is supported by National Natural Science Foundation of China (51774173), discipline innovation team of Liaoning Technical University (LNTU20TD08), LiaoNing Revitalization Talents Program (XLYC2007163) and Liaoning BaiQianWan Talents Program 2021921023 .
- There is no conflicts of interest for any author that are not apparent from their affiliations or funding.
- There is no additional information on author contributions.

Reference

Li, Z. , Gao, G. , Feng, S. , & Shi, G. . (2007). Analysis of ground vibration induced by high-speed train. Journal of Tongji University(Natural Science), 35(7), 909-914. doi:10.3321/j.issn:0253-374X.2007.07.010

Kouroussis, G. , Connolly, D. P. , & Verlinden, O. . (2014). Railway-induced ground vibrations – a review of vehicle effects. International Journal of Rail Transportation, 2(2), 69-110. doi:10.1080/23248378.2014.897791

Galvín P, Domínguez J. (2009). Experimental and numerical analyses of vibrations induced by high-speed trains on the córdoba–málaga line. Soil Dynamics & Earthquake Engineering, 29(4), 641-657. doi:10.1016/j.soildyn.2008.07.001

Takemiya, H., & Bian, X. C. (2007). Shinkansen high-speed train induced ground vibrations in view of viaduct–ground interaction. Soil Dynamics and Earthquake Engineering, 27(6),506–520. doi:10.1016/j.soildyn.2006.11.003

Li L, Peng Wentao, Li Gang,et al. (2004) Vibration induced by trains:A new seismic source and relative test. Chinese Journal of Geophysics, (04):680-684.doi:CNKI:SUN:DQWX.0.2004-04-019

Degrande, G. , & Lombaert, G. . (2000). High-speed train induced free field vibrations: in situ measurements and numerical modelling.

Degrande, G. , & Schillemans, L. . (2001). Free field vibrations during the passage of a thalys high-speed train at variable speed. Journal of Sound & Vibration, 247(1), 131-144. doi:10.1006/jsvi.2001.3718

Auersch, L. . (2006). Ground vibration due to railway traffic—the calculation of the effects of moving static loads and their experimental verification. Journal of Sound & Vibration, 293(3-5), 599-610.doi:10.1016/j.jsv.2005.08.059

Katou, M. , Matsuoka, T. , Yoshioka, O. , Sanada, Y. , & Miyoshi, T. . (2008). Numerical simulation study of ground vibrations using forces from wheels of a running high-speed train. Journal of Sound and Vibration, 318(4-5), 830-849. doi:10.1016/j.jsv.2008.04.053

F. Fuchs and G. Bokelmann, AlpArray, & Working, et al. (2017). Equidistant spectral lines in train vibrations. Seismological Research Letters, 89(1), 56-66.doi:10.1785/0220170092

Zhai, W. , Wei, K. , Song, X. , & Shao, M. . (2015). Experimental investigation into ground vibrations induced by very high speed trains on a non-ballasted track. Soil Dynamics & Earthquake Engineering, 72, 24-36. doi:10.1016/j.soildyn.2015.02.002

Zhang, G. L. , Chengjie, H. E. , Yong, L. I. , Duan, J. , Wang, T. Y. , & Zhan, Y. Z. , et al. (2019). Wavelet time function of high-speed-train seismic source and verification. Chinese Journal of Geophysics, 62(6):2344-2354.doi:CNKI:SUN:DQWX.0.2019-06-033

Wang, Z. , Ch En , C. , Li, Y. , Liu, H. , & Bai, W. . (2021). Numerical modelling for a simplified bridge pier model under high-speed train passage over the bridge. IOP Conference Series: Earth and Environmental Science,63(12):4473-4484.doi:10.1088/1755-1315/660/1/012143

Zhang, H. L. , Wang, B. L. , Ning, J. Y. , & Youming, L. I. . (2019). Interferometry imaging using high-speed-train induced seismic waves. Chinese Journal of Geophysics. 62(6):2321-2327.doi:CNKI:SUN:DQWX.0.2019-06-030

Cao J, Chen J B, (2019). Solution of green function from a moving line source and the radiation energy analysis:a simplified modeling of seismic signal induced by high-speed train. Chinese Journal of Geophysics- Chinese Edition, 62(6), 2303-2312.doi:10.6038/cjg2019M0654

Aki, K. , & Richards, P. . (2002). Quantitative Seismology. W. H. Freeman.ISBN:0716710587 (v. 1)

Wen, J. , Ning, J. , & Zhang, X. . (2019). Theoretical analysis on the characteristics of seismic wave field produced by high-speed train. Acta Scientiarum Naturalium Universitatis Pekinensis. 55(5), 10.doi:10.13209/j.0479-8023.2019.074

XK Wang, Chen, W. C. , Wen, J. C. , Ning, J. Y. , & Jiaqi, L. I. . (2019). The applications of synchrosqueezing time-frequency analysis in high-speed train induced seismic data processing. Chinese Journal of Geophysics. 62(6), 8.doi:10.6038/cjg2019M0658

Bao Qianzong, Xu Jie, Xu Mingrui. (2019). Comparative analysis of time-frequency characteristics of seismic signal induced by high-speed train. Acta Scientiarum Naturalium Universitatis Pekinensis, 2019, 55(5):805-812.doi: 10.13209/j.0479-8023.2019.076

Hu G H, Zhang G L, Sun S Y, Li Y, Yang J L, Duan J, He H B, Zhan Y Z.

(2019). Fwi of high-speed-train seismic first arrival signal. Chinese Journal of Geophysics. 62(12):4817-4824.doi:CNKI:SUN:DQWX.0.2019-12-026

Jiang Y R, Bao T Z, Ning J Y, Zhang X B. (2019). Spectral characteristic of high-speed rail seismic signal under viaduct. Acta Scientiarum Naturalium Universitatis Pekinensis.55(05):829-838.doi:10.13209/j.0479-8023.2019.072

Liu L, Jiang Y R. (2019). Attribution extraction and feature analysis for large amount of high-speed-train seismic events. Chinese Journal of Geophysics. 62(6):2313-2320.doi:CNKI:SUN:DQWX.0.2019-06-029

Jiang Y R, Liang X, Ning J Y, Bao T Z, Zhang X B. (2019). 4d ground frequency map: concept and application. Acta Scientiarum Naturalium Universitatis Pekinensis. 55(05):850-858.doi:10.13209/j.0479-8023.2019.077

Wang, X. K. , Chen, J. Y. , Chen, W. C. , Jiang, Y. R. , Bao, T. Z. , & Ning, J. Y. . (2019). Sparse modeling of seismic signals produced by high-speed trains. Chinese Journal of Geophysics.62(6):2336-2343.doi:10.6038/cjg2019M0662

He Z. X., Zhai W. M.. (2007). Ground vibration generated by high-speed trains along slab tracks. China Railway Science.28(2):7-11.doi:10.3321/j.issn:1001-4632.2007.02.002

Sheng, X. , Jones, C. , & Thompson, D. J. . (2004). A theoretical study on the influence of the track on train-induced ground vibration. Journal of Sound & Vibration, 272(3-5), 909-936.doi:10.1016/S0022-460X(03)00781-8